Acta Crystallographica Section B
**Structural
Science**
ISSN 0108-7681

In situ observation of the tetragonal–cubic phase transition in the $CeZrO_4$ solid solution – a high-temperature neutron diffraction study

Takahiro Wakita[a,b] and Masatomo Yashima[a]*

[a]Department of Materials Science and Engineering, Interdisciplinary Graduate School of Science and Engineering, Tokyo Institute of Technology, Nagatsuta-cho 4259-J2-61, Midori-ku, Yokohama 226-8502, Japan, and [b]Daiichi Kigenso Kagaku Kogyo Co. Ltd, Hirabayashi-Minami 1-6-38, Suminoe-ku, Osaka 559-0025, Japan

Correspondence e-mail:
yashima@materia.titech.ac.jp

Received 20 November 2006
Accepted 15 February 2007

The crystal structure of the compositionally homogeneous ceria–zirconia solid solution $CeZrO_4$ is refined by Rietveld analysis of neutron diffraction data measured *in situ* over the temperature range 296–1831 K. The $CeZrO_4$ exhibits a tetragonal structure with the space group $P4_2/nmc$ at temperatures from 296 to 1542 K ($Z = 1$), and a cubic fluorite-type form with the space group $Fm\overline{3}m$ at 1831 K ($Z = 2$). The isotropic atomic displacement parameters of Ce and Zr atoms B(Ce,Zr) and O atoms B(O) are found to increase with temperature, with B(O) being larger than B(Ce,Zr), suggesting the higher diffusivity of oxygen ions. The ratio of the c axial length to the a length of the pseudo-fluorite lattice (c/a_F axial ratio) for the tetragonal $CeZrO_4$ phase increased from 296 to 1034 K and decreased from 1291 to 1542 K, reaching unity between 1542 and 1831 K. The displacement of O atoms along the c axis in the tetragonal $CeZrO_4$ phase increased from 296 to 1034 K and decreased from 1291 to 1542 K, reaching 0.0 Å between 1542 and 1831 K. These results indicate that the cubic-to-tetragonal phase transition between 1542 and 1831 K is accompanied by oxygen displacement along the c axis and the increase of the c/a_F axial ratio from unity.

1. Introduction

Materials containing ceria and zirconia have become the focus of intense study in recent years as a result of several applications in the field of high-temperature materials for technologies such as fuel cells, oxygen gas sensors (Inaba & Tagawa, 1996) and structural ceramics (Tsukuma & Shimada, 1985), and as components of automotive exhaust catalysts for the removal of noxious compounds (Yao & Yao, 1984; Ozawa *et al.*, 1993; Murota *et al.*, 1993; Trovarelli, 1996). The material properties of these compounds are strongly dependent on the crystal structure and phase, yet the form of these compounds at high temperature, at which most function most efficiently, remains poorly understood. In the case of the $Ce_{1-x}Zr_xO_2$ solid solutions, there is strong interest in the compositionally homogeneous metastable forms of the tetragonal phase, since these materials are used extensively as promoters in three-way catalysts for automotive exhausts. The compositional dependence of the phase and crystal structure of compositionally homogeneous metastable $Ce_{1-x}Zr_xO_2$ solid solutions have been investigated by many researchers (Meriani, 1985; Yashima *et al.*, 1993*a*,*b*; Yashima, Arashi, Kakihana & Yoshimura, 1994; Yashima, Takashina, Kakihana & Yoshimura, 1994; Yashima, Ohtake, Kakihana, Arashi & Yoshimura, 1996; Yashima *et al.*, 1998; Omata *et al.*, 1999; Kaspar & Fornasiero, 2003; Enzo *et al.*, 2000; Lamas *et al.*, 2005; Zhang *et al.*, 2006). As the compositionally homogeneous $CeZrO_4$ solid solution also exhibits high catalytic performance in the $Ce_{1-x}Zr_xO_2$ (Trovarelli *et al.*, 1997; Suda *et al.*, 2001), it is therefore important to investigate the crystal structure and phase transition in the $CeZrO_4$ solid solution at high temperatures.

The crystal structure of the compositionally homogeneous $Ce_{1-x}Zr_xO_2$ solid solutions has been studied by Yashima *et al.* (1993*a*,*b*), Yashima, Arashi, Kakihana & Yoshimura (1994), Yashima, Takashina, Kakihana & Yoshimura (1994) and Yashima *et al.* (1998), who have reported three forms of the tetragonal phase (t, t', t''), all belonging to the space group $P4_2/nmc$. The stable form of the tetragonal phase is called the t form and is restricted to the solubility limit in the equilibrium phase diagram (Yashima *et al.*, 1993*a*,*b*; Yashima, Arashi, Kakihana & Yoshimura, 1994; Yashima, Takashina, Kakihana & Yoshimura, 1994). The t' form is metastable and unstable compared with the coexistence of the t form and cubic (c) phase. The t' form has an axial ratio larger than unity, that is, $c_{t'}/(2^{1/2}a_{t'}) > 1$, where $c_{t'}$ and $a_{t'}$ are the unit-cell parameters c and a of the t' form (Fig. 1). The t'' form is another metastable tetragonal phase with an axial ratio of unity $[c_{t'}/(2^{1/2}a_{t'}) = 1]$. The t'' form is designated as a tetragonal symmetry owing to the displacement of O atoms along the c axis from the regular position in the cubic phase (Fig. 1).

Yashima *et al.* (1993*b*) investigated the temperature dependence of the $c_{t'}/(2^{1/2}a_{t'})$ ratio in the $CeZrO_4$ solid solution by *ex situ* X-ray diffraction measurements of quenched samples at room temperature. In the present work the temperature dependence of the unit-cell parameters and axial ratio of the $CeZrO_4$ solid solution are investigated by *in situ* neutron diffraction measurements at high temperatures. Yashima and co-workers (Yashima, Arashi, Kakihana & Yoshimura, 1994; Yashima, Takashina, Kakihana & Yoshimura, 1994; Yashima *et al.*, 1998) suggested that the cubic-to-tetragonal phase transition is induced by the displacement of O atoms (Fig. 1) on the basis of the high-temperature Raman spectra of $Ce_{0.8}Zr_{0.2}O_2$ and *ex situ* neutron and synchrotron powder diffraction data for $Ce_{1-x}Zr_xO_2$ (x = 0.1, 0.2, 0.3, 0.35, 0.4 and 0.5) obtained at room temperature. As no high-temperature *in situ* studies of the crystal structure or cubic–tetragonal phase transition have been conducted for the $CeZrO_4$ solid solution, the temperature dependence of the oxygen displacement and atomic displacement parameters remains an unresolved issue. Through the investigation of the temperature dependence of the unit-cell parameters, the axial ratio $c_{t'}/(2^{1/2}a_{t'})$, positional and atomic displacement parameters, and oxygen displacement of the $CeZrO_4$ solid solution, it is demonstrated in this study for the first time that the c–t' transition between 1542 and 1831 K is accompanied by oxygen displacement along the c axis and an increase in the c/a_F axial ratio from unity.

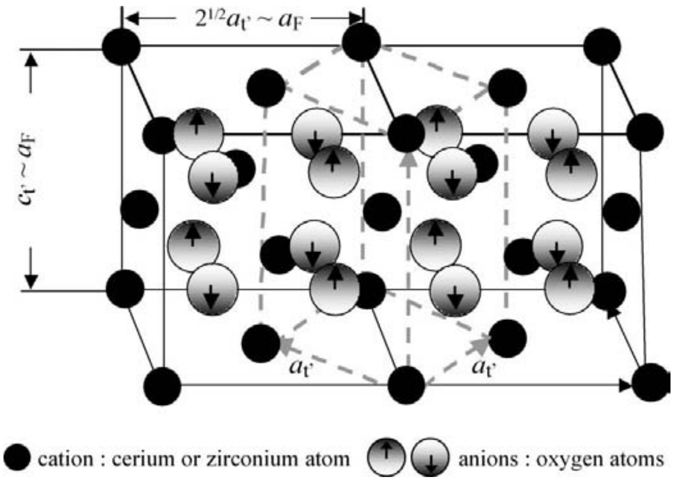

Figure 1
Crystal structure of metastable tetragonal (t') $CeZrO_4$ solid solution and relationship between tetragonal cell and pseudo-cubic fluorite (F) cell. Filled and shaded circles denote cations and anions, respectively. Arrows denote the displacement of O atoms along the c axis. Thick dashed lines denote the primitive cell after Teufer (1962), and thin solid lines delineate two pseudo-fluorite cells.

2. Experiments and data analysis

Fig. 2 shows the synthesis procedure of $CeZrO_4$ powders and pellets. $Ce(NO_3)_3$ (99.9% purity) and $ZrO(NO_3)_2$ (99.9% purity) aqueous solutions were supplied from Daiichi Kigenso Kagaku Kogyo Co. Ltd. These solutions were mixed at an atomic ratio of Zr:Ce = 1:1 and added to a 5 mass % ammonia aqueous solution, resulting in the formation of hydroxides containing Ce and Zr species. The resultant

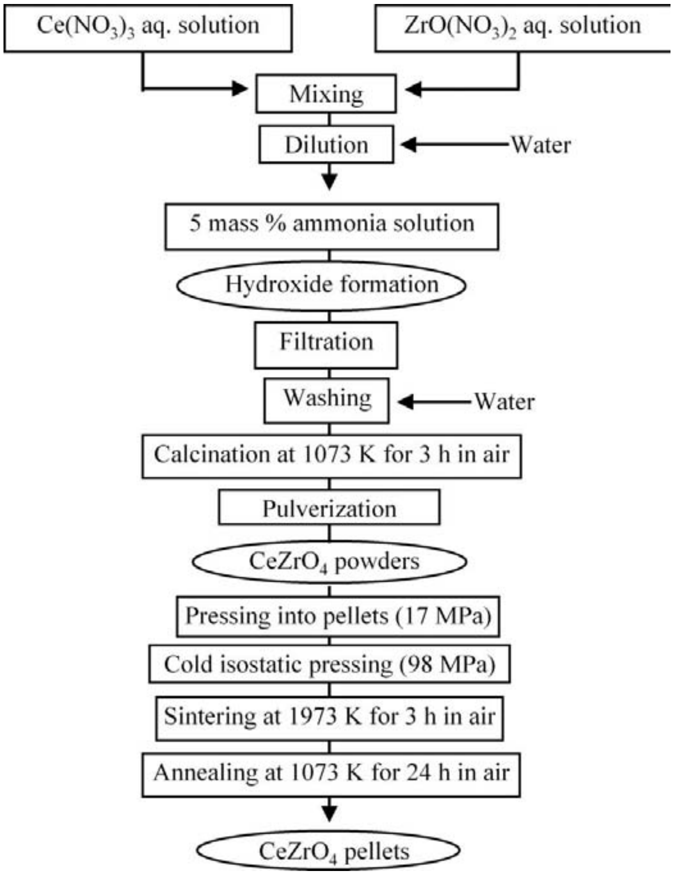

Figure 2
Synthesis procedure for $CeZrO_4$ pellets.

precipitates were washed after filtration and then calcined at 1073 K for 3 h. The $CeZrO_4$ powders thus obtained were pressed uniaxially at 17 MPa, and then pressed isostatically into pellets at 98 MPa. The pellets were sintered at 1973 K for 5 h in air and then annealed at 1073 K for 24 h in air to afford a cylindrical product of 19 mm in diameter and 76 mm in height. The $CeZrO_{4-\delta}$ solid solution thus obtained was pale yellow, indicating the stoichiometry to be $\delta = 0$, where δ denotes the proportion of oxygen vacancies. Chemical analysis by inductively coupled plasma optical-emission spectroscopy (ICP-OES) indicated a small amount of hafnium, corresponding to an average chemical composition of $Ce_{0.4943\,(3)}(Zr_{0.993\,(2)}Hf_{0.007\,(2)})_{0.5057\,(3)}O_2$, where the values in parentheses denote the error bar in the last digit.

Neutron powder diffraction measurements were performed in air using a 150 detector HERMES system (Ohoyama *et al.*, 1998) installed at the JRR-3M reactor of the Japan Atomic Energy Agency, Tokai, Japan. Neutrons with wavelength of 1.81430 (7) Å were obtained from the (311) reflection of a Ge monochromator. Diffraction data were collected in the 2θ range 5–155° at intervals of 0.1° over the temperature range 296–1831 K. A furnace equipped with $MoSi_2$ heaters (Yashima, 2002) was used for the high-temperature neutron diffraction measurements. Sample temperatures were maintained constant during data acquisition.

The crystal structures of the $CeZrO_4$ material were refined by the Rietveld method using the computer program *RIETAN*-2000 (Izumi & Ikeda, 2000). The peak shape was assumed to be a modified split-type pseudo-Voigt function and a cut-off value of 7.00 (Toraya, 1990). The background was approximated by a 12-parameter polynomial in $2\theta^n$ ($n = 0$–11). The n parameters were refined simultaneously with the unit-cell, zero-point scale, profile-shape and crystal structural parameters.

3. Results

Figs. 3 and 4 show the neutron diffraction profiles of the $CeZrO_4$ solid solution measured at 296, 1542 and 1831 K. All reflections are indexed by a tetragonal cell ($P4_2/nmc$) between 296 and 1542 K. The peak splitting between the $004_{t'}$ and $220_{t'}$ reflections was clearly observed between 296 and 1542 K (Figs. 3*a* and *b*). Here $hkl_{t'}$ denotes the hkl reflection of the t' form. The $102_{t'}$ reflection was clearly detected in this temperature range (Fig. 4), allowing the $CeZrO_4$ solid solution to be identified as the single phase of the t' form with an axial ratio $c_{t'}/(2^{1/2}a_{t'})$ larger than unity $[c_{t'}/(2^{1/2}a_{t'}) > 1]$ at temperatures between 296 and 1542 K. All reflections in the neutron diffraction profile measured at 1831 K are indexed by a cubic fluorite-type cell ($Fm\bar{3}m$; Fig. 3*c*). The 400_c reflection exhibits a single feature without splitting between the $004_{t'}$ and $220_{t'}$ reflections. No $102_{t'}$ reflection was detected at 1831 K (Fig. 4*c*).

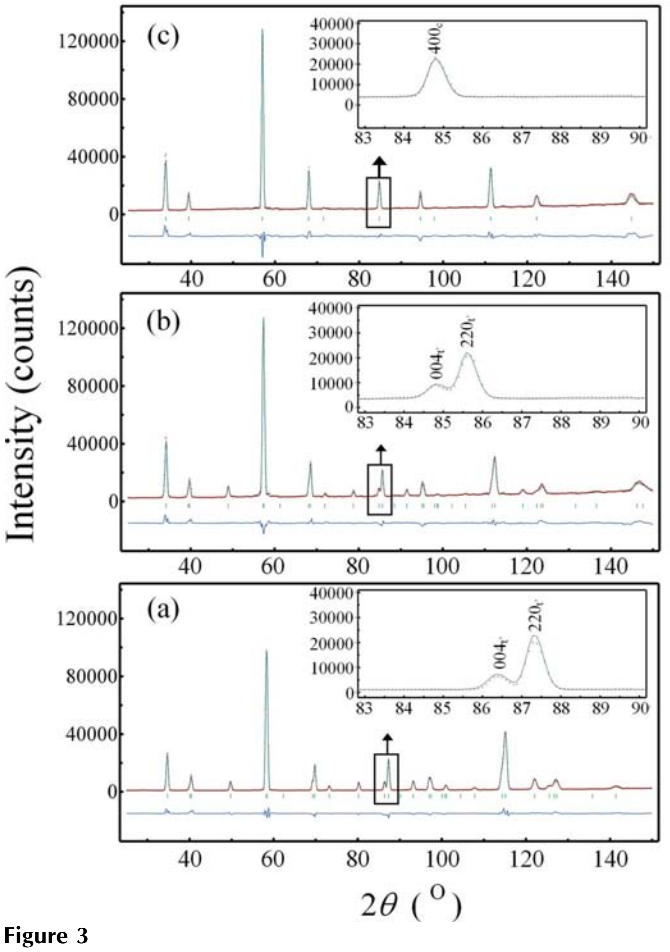

Figure 3
Rietveld fitting patterns for neutron diffraction data of $CeZrO_4$ solid solution measured at (*a*) 296, (*b*) 1542 and (*c*) 1831 K. Crosses and lines denote observed and calculated intensities, respectively. Short vertical lines indicate the positions of possible Bragg reflections of (*a*), (*b*) tetragonal and (*c*) cubic $CrZrO_4$ phases. Lines below the profiles denote the difference between observed and calculated intensities.

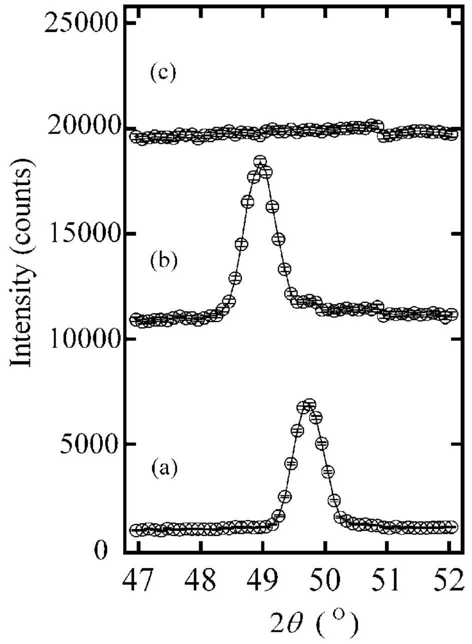

Figure 4
Neutron diffraction profiles around the $102_{t'}$ reflection of $CeZrO_4$ solid solution measured at (*a*) 296, (*b*) 1542 and (*c*) 1831 K.

Table 1
Crystal parameters and reliability factors of Rietveld analysis of $CeZrO_4$ solid solution measured at different temperatures.

$M_r = 295.40$, $\theta_{\rm min} = 25°$, $\theta_{\rm max} = 150°$.

Temperature (K)		296	507	772	1034	1291	1542	1831
Space group		$P4_2/nmc$	$P4_2/nmc$	$P4_2/nmc$	$P4_2/nmc$	$P4_2/nmc$	$P4_2/nmc$	$Fm\bar{3}m$
Unit-cell parameters	a (Å)	3.7191 (2)	3.7286 (2)	3.7386 (3)	3.7503 (3)	3.7640 (3)	3.7781 (4)	5.3848 (6)
	c (Å)	5.3057 (4)	5.3215 (4)	5.3381 (4)	5.3564 (5)	5.3745 (5)	5.3833 (7)	
Ce, Zr	B (Å^2)†	0.62 (4)	0.90 (4)	1.15 (4)	1.58 (5)	2.07 (5)	2.61 (7)	2.49 (6)
O	g (O)	1.0	1.0	1.0	1.0	1.0	1.0	1.0
	B (Å^2)†	1.18 (3)	1.59 (4)	2.01 (4)	2.63 (5)	3.49 (6)	4.64 (7)	6.05 (8)
	z (O)‡	0.2190 (2)	0.2184 (2)	0.2179 (2)	0.2170 (2)	0.2170 (2)	0.2199 (3)	0.25
Reliability factors in the Rietveld analysis	$R_{\rm wp}$§	0.0879	0.0787	0.0834	0.0749	0.0685	0.0720	0.0821
	$R_{\rm p}$§	0.0628	0.0573	0.0618	0.0563	0.0514	0.0551	0.0605
	GoF§	4.91	4.40	4.70	4.74	4.88	5.69	6.40
	$R_{\rm I}$§	0.0483	0.0512	0.0587	0.0553	0.0562	0.0582	0.0797
	R_F§	0.0325	0.0350	0.0394	0.0353	0.0343	0.0378	0.0441
V (Å^3)		73.39 (1)	73.98 (1)	74.61 (1)	75.34 (1)	76.14 (1)	76.84 (2)	156.13 (3)
Z		1	1	1	1	1	1	2
No. of parameters		32	32	32	32	32	32	27

† B: isotropic atomic displacement parameter. ‡ z(O): fractional coordinate z of O atoms. § Standard Rietveld agreement index (Young *et al.*, 1982).

Thus, the $CeZrO_4$ solid solution at 1831 K is identified as having a cubic structure. No impurity phases were detected in the neutron diffraction profiles between 296 and 1831 K. Each peak did not exhibit anisotropic peak broadening. These results indicate that the CeO_2 composition in the sample is homogeneous in the whole temperature range. The t' form is metastable and unstable compared with the stable $t + c$ two-phase coexistence. The stable t and c phases did not form, because the heating rate (*ca* 10 K min^{-1}) was too high and the measurement time (*ca* 90 min) was too short for the phase separation to occur.

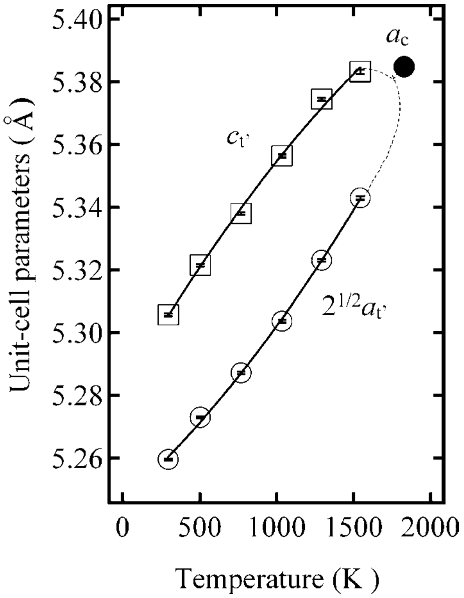

Figure 5
Temperature dependence of the unit-cell parameters of $CeZrO_4$ solid solution. Open circles and squares denote the unit-cell parameters $2^{1/2}a_{t'}$ and $c_{t'}$ of the metastable tetragonal t' form, respectively. The filled circle denotes the unit-cell parameter a_c of the cubic phase. Error bars of standard uncertainties in the Rietveld analysis are smaller than the datum symbols. The solid line is the least-squares fit (quadratic polynomial) and the dashed line is a guide to the eye.

Rietveld analysis of the $CeZrO_4$ solid solution was carried out for the tetragonal structure with the $P4_2/nmc$ space group ($Z = 1$) at 296–1542 K, where the cation (Ce^{4+} and Zr^{4+}) and anion (O^{2-}) were placed at the special positions of 2(a) 0,0,0 and 4(d) 0,1/2,z, respectively. Data at 1831 K were analyzed assuming the cubic fluorite-type structure with the space group $Fm\bar{3}m$ ($Z = 2$), where the cation (Ce^{4+} and Zr^{4+}) and anion (O^{2-}) were placed at 4(a) 0,0,0 and 8(c) 1/4,1/4,1/4, respectively. In a preliminary analysis, the occupancy factor of the O atom g(O) was refined. The refined g(O) was unity

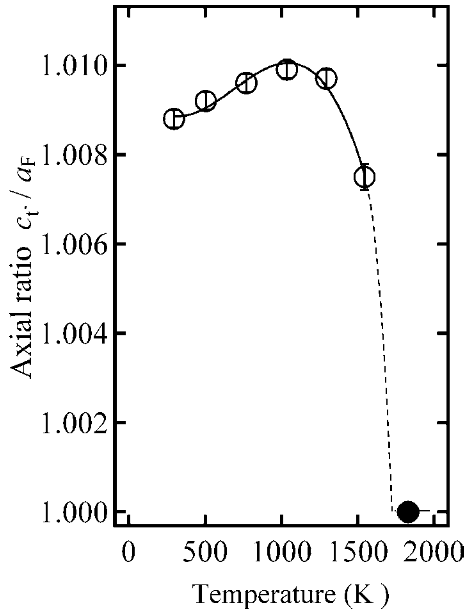

Figure 6
Relationship between temperature and axial ratio $c_{t'}/a_F$ for $CeZrO_4$ solid solution. Open and filled circles denote the $c_{t'}/a_F$ ratios of the t' and c phases, respectively. The solid line is a least-squares fit (polynomial) and the dashed line is a guide to the eye.

within the error bar, thus we fixed the $g(\mathrm{O})$ to be unity in the final refinement. The calculated profile is in good agreement with the observed data (Fig. 3). Table 1[1] lists the crystal parameters and reliability factors in the Rietveld analyses of the neutron diffraction data for the $\mathrm{CeZrO_4}$ solid solution between 296 and 1831 K. The refined axial ratio $c_{t'}/(2^{1/2}a_{t'})$ at room temperature was 1.0088 (1), consistent with that reported previously (Yashima *et al.*, 1998). The refined fractional coordinate z of oxygen atoms $z(\mathrm{O})$ was 0.2189 (2) at room temperature, which is also consistent with the results of Yashima *et al.* (1998) and Lamas *et al.* (2005) within ±3 standard deviations (σ) of $z(\mathrm{O})$.

The unit-cell parameters a and c of the $\mathrm{CeZrO_4}$ solid solution increased with temperature, coinciding between 1542 and 1831 K because of the t'–c transformation (Fig. 5). The axial ratio $c_{t'}/(2^{1/2}a_{t'})$ of the metastable t'-$\mathrm{CeZrO_4}$ increased slightly from 296 to 1034 K, and decreased from 1291 to 1542 K (Fig. 6). The axial ratio became unity between 1542 and 1831 K, corresponding to the t'–c phase transition. The fractional coordinate $z(\mathrm{O})$ of $\mathrm{CeZrO_4}$ decreased from 296 to 1034 K, and increased from 1291 K, reaching 1/4 between 1542 and 1831 K (Fig. 7). The oxygen displacement $d(\mathrm{O})$ from the regular $8(c)$ position of the cubic fluorite-type structure can be estimated by the equation $d(\mathrm{O}) = c[0.25 - z(\mathrm{O})]$. The $d(\mathrm{O})$ value of $\mathrm{CeZrO_4}$ increased slightly from 296 to 1034 K, and then decreased to 0.0 Å between 1542 and 1831 K (Fig. 8), corresponding to the t'–c phase transition. The isotropic atomic displacement parameters of Ce and Zr atoms $B(\mathrm{Ce,Zr})$ and O atoms $B(\mathrm{O})$ increased with temperature (Fig. 9). $B(\mathrm{O})$ was larger than $B(\mathrm{Ce,Zr})$, suggesting the higher diffusivity of oxygen ions. This is consistent with the relation of $B(\mathrm{Ce,Zr}) < B(\mathrm{O})$ in $\mathrm{Ce_{1-x}Zr_xO_2}$ at room temperature (Lamas *et al.*, 2005) and the diffusivity experiments in the literature (Yashima *et al.*, 1993*a*; Yashima, Kakihara & Yoshimura, 1996).

4. Discussion

The present work based on *in situ* experiments has demonstrated that the c–t' phase transition of the $\mathrm{CeZrO_4}$ solid solution occurs between 1542 and 1831 K (Figs. 3–8). The c–t' transition temperature between 1542 and 1831 K is consistent with the previous *ex situ* study (Yashima *et al.*, 1993*b*). The $c_{t'}/(2^{1/2}a_{t'})$ value is 1.0 for the cubic phase and increases with decreasing temperature below the c–t' phase transition temperature. This indicates that the c–t' phase transition is accompanied by the increase of c/a_F ratio from unity. The present *in situ* experiments also revealed the temperature dependence of the atomic coordinate $z(\mathrm{O})$ and oxygen displacement $d(\mathrm{O})$ for the first time (Figs. 7 and 8). The $d(\mathrm{O})$ value is 0.0 Å for the cubic phase and increases with decreasing temperature below the c–t' phase-transition temperature. This indicates that the c–t' phase transition is accompanied by oxygen displacement. Yashima *et al.* suggested oxygen-induced structural change as a mechanism for the c–t' transformation in $\mathrm{ZrO_2}$–$\mathrm{CeO_2}$ systems (Yashima *et al.*, 1993*a*,*b*; Yashima, Arashi, Kakihana & Yoshimura, 1994; Yashima, Takashina, Kakihana & Yoshimura, 1994; Yashima

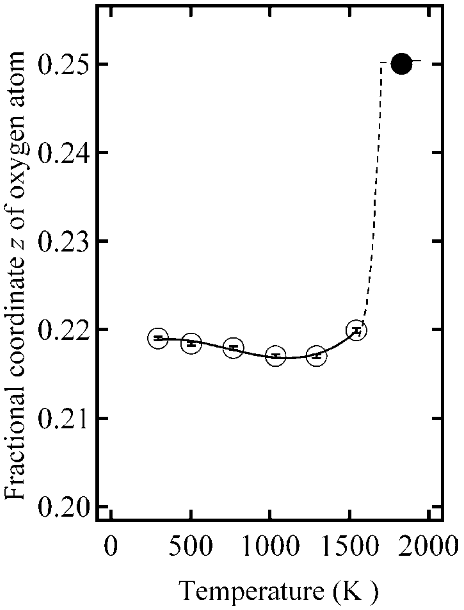

Figure 7
Temperature dependence of the fractional coordinate z of O atoms in $\mathrm{CeZrO_4}$ solid solution. Open circles denote t'-$\mathrm{CeZrO_4}$ and the solid circle denotes c-$\mathrm{CeZrO_4}$. Error bars denote the standard uncertainties in the Rietveld analysis. The solid line is a least-squares fit (polynomial) and the dashed line is a guide to the eye.

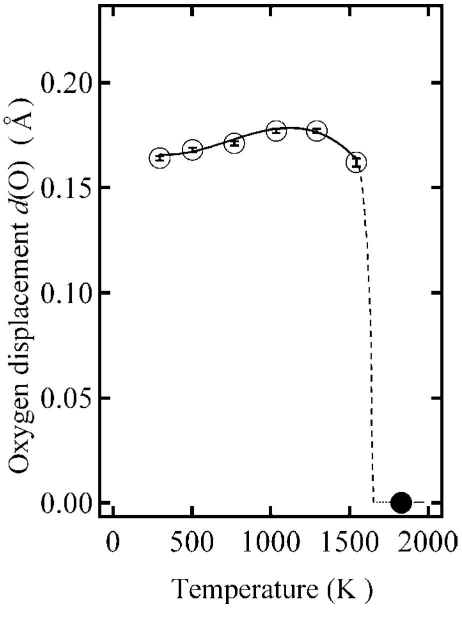

Figure 8
Temperature dependence of the oxygen displacement of $\mathrm{CeZrO_4}$ solid solution. Open circles denote t'-$\mathrm{CeZrO_4}$ and the solid circle denotes c-$\mathrm{CeZrO_4}$. Error bars were estimated from the standard uncertainties of c and z obtained in the Rietveld analysis. The solid line is a least-squares fit (polynomial) and the dashed line is a guide to the eye.

---

[1] Supplementary data for this paper are available from the IUCr electronic archives (Reference: OG5020). Services for accessing these data are described at the back of the journal.

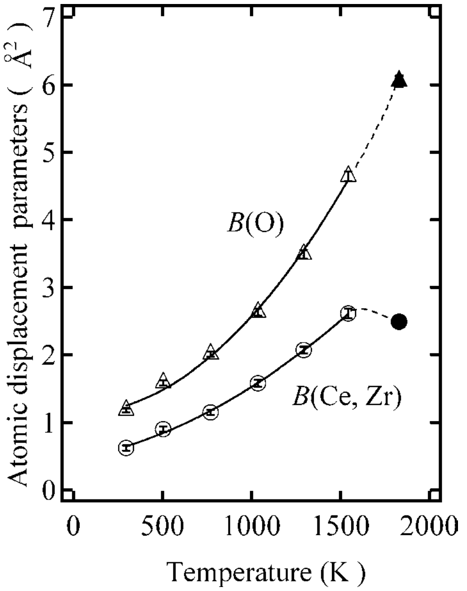

Figure 9
Temperature dependence of isotropic atomic displacement parameters of Ce and Zr atoms [B(Ce, Zr)] and O atoms [B(O)] in $CeZrO_4$ solid solution. Open circles denote B(Ce,Zr) and triangles denote B(O) for t'-$CeZrO_4$. Filled symbols denote c-$CeZrO_4$. The solid line is a least-squares fit (quadratic polynomial) and the dashed line is a guide to the eye.

et al., 1998) and ZrO_2–$RO_{1.5}$ (R = Y, Nd, Sm, Er, Yb) systems (Yashima, Ohtake, Kakihana, Arashi & Yoshimura, 1996) on the basis of data acquired at room temperature. Yashima, Arashi, Kakihana & Yoshimura (1994) also suggested such oxygen-induced behavior in the ZrO_2–CeO_2 system through *in situ* Raman studies. The present work has provided direct evidence of the temperature dependence of oxygen displacement d(O) as an oxygen-induced structural change responsible for the c–t' transition.

5. Conclusions

The crystal structure of the compositionally homogenous $CeZrO_4$ solid solution was investigated by *in situ* neutron powder diffraction analysis and Rietveld refinement over a temperature range of 296 to 1831 K. The $CeZrO_4$ solid solution was found to transform from the tetragonal t' phase to the cubic phase between 1542 and 1831 K, accompanied by an increase in the isotropic atomic displacement parameters B(Ce,Zr) and B(O) with increasing temperature. B(O) was found to be larger than B(Ce,Zr), suggesting a higher diffusivity of oxygen ions. The axial ratio c/a_F of the tetragonal $CeZrO_4$ phase increased from 296 to 1034 K and decreased from 1291 to 1542 K, reaching unity between 1542 and 1831 K. The displacement of O atoms along the c axis in the tetragonal $CeZrO_4$ phase increased from 296 to 1034 K and decreased from 1291 to 1542 K, reaching 0.00 between 1542 and 1831 K. These results indicate that the tetragonal-to-cubic phase transition is accompanied by oxygen displacement along the c axis and the increase of the c/a_F axial ratio from unity.

This research was supported in part by the Ministry of Education, Culture, Sport, Science and Technology of Japan through a Grant-in-Aid for Scientific Research (B). The authors would like to thank to Dr K. Ohoyama and Mr K. Nemoto (Tohoku University) for facilitating neutron diffraction measurements, and Dr R. Ali (National Institute for Materials Science), Mr Y. Ando, Mr T. Tsuji, Mr Q. Xu, Mr T. Ueda and Mr Y. Kawaike (Tokyo Institute of Technology) for experimental assistance in the neutron powder diffraction measurements.

References

Enzo, S., Delogu, F., Frattini, R., Primavera, A. & Trovarelli, A. (2000). *J. Mater. Res.* **15**, 1538–1545.
Inaba, H. & Tagawa, H. (1996). *Solid State Ion.* **83**, 1–16.
Izumi, F. & Ikeda, T. (2000). *Mater. Sci. Forum*, **321–324**, 198–203.
Kaspar, J., Fornasiero, P., Balducci, G., DiMonte, R., Hickey, N. & Sergo, V. (2003). *Inorg. Chim. Acta*, **349**, 217–226.
Lamas, D. G., Fuentes, R. O., Fabregas, I. O., Fernandez de Rapp, M. E., Lascalea, G. E., Casanova, J. R., Walsoe de Reca, N. E. & Craievich, A. F. (2005). *J. Appl. Cryst.* **38**, 867–873.
Meriani, S. (1985). *J. Mater. Sci. Eng.* **71**, 369–370.
Murota, T., Hasegawa, T., Aozasa, S., Matsui, H. & Motoyama, M. (1993). *J. Alloys Compd.* **193**, 298–299.
Ohoyama, K., Kanouchi, T., Nemoto, K., Ohashi, M., Kajitani, T. & Yamaguchi, Y. (1998). *Jpn. J. Appl. Phys.* **37**, 3319–3326.
Omata, T., Kishimoto, H., Otsuka-Yao-Matsuo, S., Ohtori, N. & Umesaki, N. (1999). *J. Solid State Chem.* **147**, 573–583.
Ozawa, M., Kimura, M. & Isogai, A. (1993). *J. Alloys Compd.* **193**, 73–75.
Suda, A., Sobukawa, H., Suzuki, T., Kandori, T., Ukyo, Y. & Sugiura, M. (2001). *J. Ceram. Soc. Jpn*, **109**, 177–180.
Teufer, G. (1962). *Acta Cryst.* **15**, 1187.
Toraya, H. (1990). *J. Appl. Cryst.* **23**, 485–491.
Trovarelli, A. (1996). *Catal. Rev. Sci. Eng.* **38**, 439–520.
Trovarelli, A., Zamar, F., Llorca, J., Leitenburg, C., Dolcetti, G. & Kiss, J. T. (1997). *J. Catal.* **169**, 490–502.
Tsukuma, K. & Shimada, M. (1985). *J. Mater. Sci.* **20**, 1178–1184.
Yao, H. C. & Yao, T. F. Yu (1984). *J. Catal.* **86**, 254–265.
Yashima, M. (2002). *J. Am. Ceram. Soc.* **85**, 2925–2930.
Yashima, M., Arashi, H., Kakihana, M. & Yoshimura, M. (1994). *J. Am. Ceram. Soc.* **77**, 1067–1071.
Yashima, M., Kakihana, M. & Yoshimura, M. (1996). *Solid State Ion.* **86–88**, 1131–1149.
Yashima, M., Morimoto, K., Ishizawa, N. & Yoshimura, M. (1993*a*). *J. Am. Ceram. Soc.* **76**, 1745–1750.
Yashima, M., Morimoto, K., Ishizawa, N. & Yoshimura, M. (1993*b*). *J. Am. Ceram. Soc.* **76**, 2865–2868.
Yashima, M., Ohtake, K., Kakihana, M., Arashi, H. & Yoshimura, M. (1996). *J. Phys. Chem. Solids*, **57**, 17–24.
Yashima, M., Sasaki, S., Yamaguchi, Y., Kakihana, M., Yoshimura, M. & Mori, T. (1998). *Appl. Phys. Lett.* **72**, 182–184.
Yashima, M., Takashina, H., Kakihana, M. & Yoshimura, M. (1994). *J. Am. Ceram. Soc.* **77**, 1869–1874.
Young, R. A., Prince, E. & Sparks, R. A. (1982). *J. Appl. Cryst.* **15**, 357–359.
Zhang, F., Chen, C.-H., Hanson, J. C., Robinson, R. D., Herman, I. P. & Chan, S.-W. (2006). *J. Am. Ceram. Soc.* **89**, 1028–1036.